

Effect of General Relativity and rotation on the energy deposition rate for $\nu + \bar{\nu} \rightarrow e^+ + e^-$ inside a compact star

Abhijit Bhattacharyya*

Department of Physics, University of Calcutta, 92, A. P. C. Road; Kolkata - 700009; INDIA

Sanjay K. Ghosh,[†] Ritam Mallick,[‡] and Sibaji Raha[§]
*Centre for Astroparticle Physics and Space Science & Department of
 Physics; Bose Institute; 93/1, A.P.C Road; Kolkata - 700009; INDIA*

We have studied the $\nu + \bar{\nu} \rightarrow e^+ + e^-$ energy deposition rate in a rotating compact star. This reaction is important for the study of gamma ray bursts. The General Relativistic (GR) effects on the energy deposition rate have been incorporated. We find that the efficiency of the process is larger for a rotating star. The total energy deposition rate increases by more than an order of magnitude due to rotation. The dependence of this energy deposition rate on the deformation parameter of the star has also been discussed.

PACS numbers: 26.60.+c

I. INTRODUCTION

Gamma Ray Burst (GRB) and its possible connection with neutrino production in compact stars is a field of high current interest. GRBs were first discovered in the late 1960s by U.S. military satellites [1]. Until recently, GRBs were perhaps the biggest mystery in high energy astronomy. To unravel this mystery, several satellite based detectors have been employed for the observation of GRB. GRBs are separated in two classes; long duration bursts (long GRB) which last from 2 sec. to several minutes, with average duration of 30 seconds and short duration bursts (short GRB) with burst duration from few milliseconds to 2 seconds, average being 0.3 seconds [2].

Initial evidence that the long GRBs are associated with supernovae came from the study of GRB 980425 in 1998 [3]. This burst was tentatively linked to supernova SN 1998bw. The definitive proof came on March 29, 2003, when a relatively nearby burst, GRB 030329, produced an afterglow whose optical spectrum was nearly identical to a supernova [4]. In contrast, there is a scarcity of information on short GRBs. Until recently, information was only available about the burst; the post-burst picture was not clear. Of late, the detection of afterglows in short GRBs and also precise localizations of different short GRBs have provided some more inputs for the study of these phenomena.

On the otherhand, compact stars (neutron or quark stars) are objects formed in the aftermath of supernova. The central density of these stars can be as high as 10 times that of normal nuclear matter. Due to beta equilibration, a large number of neutrinos and antineutrinos may be produced inside the compact stars. These neutrinos and antineutrinos could annihilate and give rise to electron-positron pairs through the reaction $\nu\bar{\nu} \rightarrow e^+e^-$. These e^+e^- pairs may further give rise to gamma rays which could be a possible explanation of the observed GRBs. Hence it is very important to study the energy deposition in the $\nu\bar{\nu}$ annihilation process.

Previous calculation of this reaction in the vicinity of a neutron star has been based on newtonian gravity [5, 6], *i.e.* $(2GM/c^2R) \ll 1$, where M is the gravitational mass of the neutron star and R is the distance scale. The effect of gravity was incorporated in refs. [7, 8], but only for a static star. In our present calculation, we extend the basic premise to rotating stars.

In this work first we will discuss the equation of state (EOS), the metric and the structure of the star. The effect of GR and also that of rotation will be discussed next and finally we will present our results.

*Electronic address: abphy@caluniv.ac.in

[†]Electronic address: sanjay@bosemain.boseinst.ac.in

[‡]Electronic address: ritam@bosemain.boseinst.ac.in

[§]Electronic address: sibaji@bosemain.boseinst.ac.in

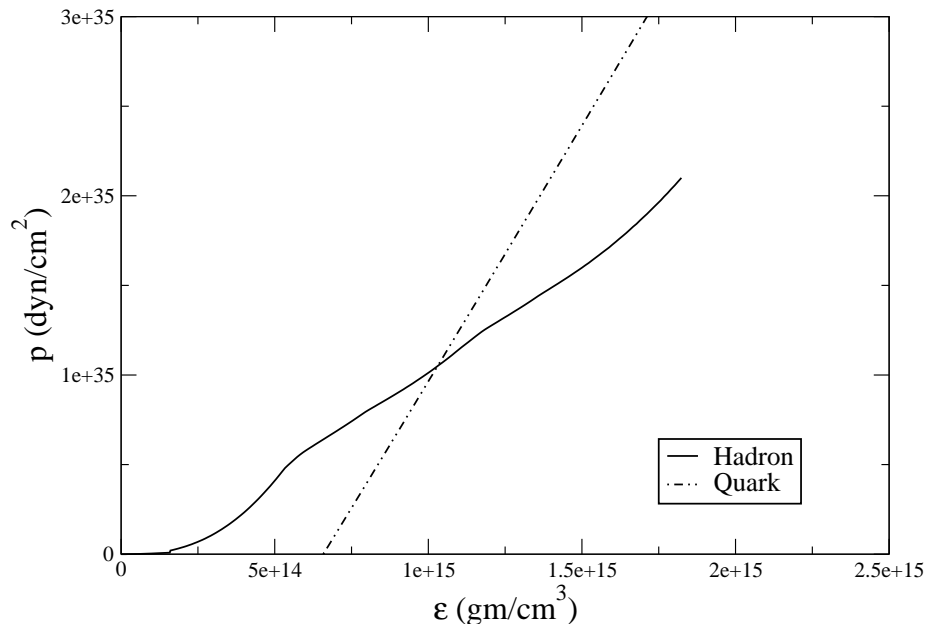


FIG. 1: Variation of pressure with energy is plotted for both hadronic and quark EOS.

II. STAR STRUCTURE

The structure of the star is described by the metric given by [9]

$$ds^2 = -e^{\gamma+\rho} dt^2 + e^{2\alpha} (dr^2 + r^2 d\theta^2) + e^{\gamma-\rho} r^2 \sin^2\theta (d\phi - \omega dt)^2 \quad (1)$$

The four gravitational potentials, namely α, γ, ρ and ω are functions of θ and r only. Once these potentials are known, the observed properties of the star can be evaluated. The Einstein's equations for the three potentials γ, ρ and ω have been solved using Green's function technique [10, 11]. The fourth potential α has been determined from other potentials. All the potentials have been solved for both static as well as rotating stars using the 'rns' code; the details of the code may be obtained in ref. [12].

The solution of the Einstein's equations needs an EOS as an input. In the present work we have used a non-linear version of the Walecka model with TM1 [13] parameter set. For comparison, we have also used a quark matter EOS obtained from standard Bag model with $B^{1/4} = 160 \text{ MeV}$. These EOSs have been plotted in figure 1. The quark matter EOS is more stable at higher energy densities. Using these EOSs, we can get the structure of the star by solving the Einstein's equations. The solution of Einstein's equations also provide the density profiles of the star. These profiles, for a star rotating in the mass shedding limit i.e. with the Keplerian velocity, are plotted in fig. 2 and fig. 3. The neutrino annihilation process has been studied for both neutron and quark stars with the central energy density $1.2 \times 10^{15} \text{ gm/cm}^3$. Fig. 2 shows the variation of energy density with the radius of the star for $\chi = \cos\theta = 0$, i.e. along the equator. Here θ is the angle that radius vector makes with the polar axis. From fig 2. we can see that the energy density is high at the centre of the star, and as we move radially outwards the energy density decreases to a lower value. Fig. 3 shows the variation of the energy density with χ . This is plotted for radius $r = 3.5 \text{ Km}$ from the centre of the star. The curve shows that for $\chi = 0$, i.e. at the equator, the energy density is maximum and it falls off gradually as we approach the pole $\chi = 1$. We would like to mention at this stage that for the hadronic matter we have considered a thin crust. On the other hand, quark matter being self bound, no such crust has been used as for quark star. Hence the energy density at the surface of a quark star is much higher compared to that of a hadronic star (fig. 2).

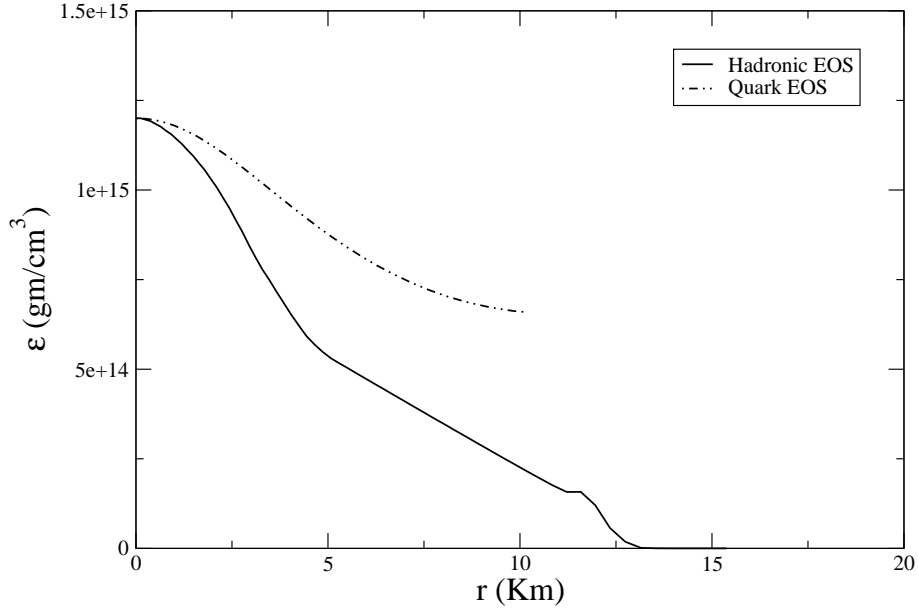


FIG. 2: Variation of energy density along the equator of the star which is rotating with the Keplerian velocity.

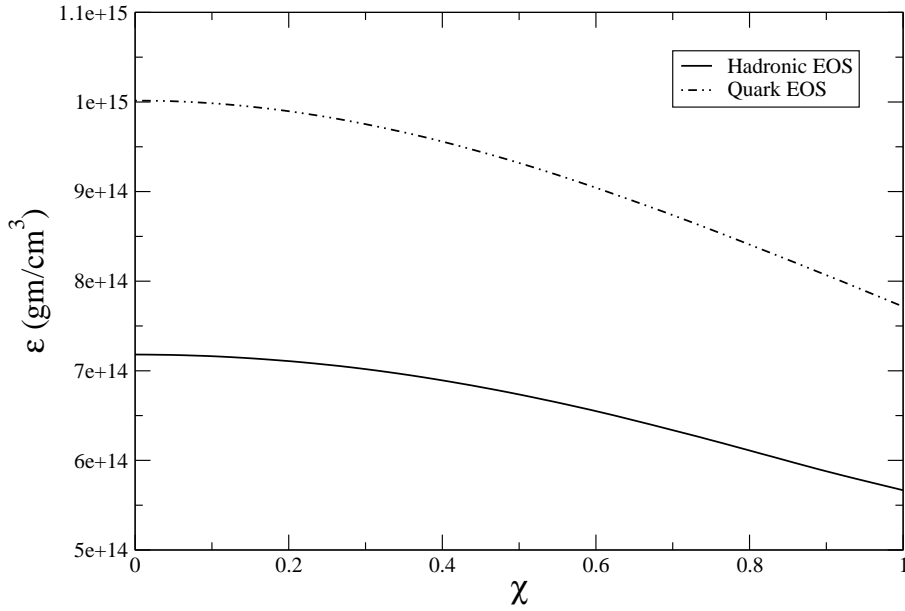


FIG. 3: Variation of energy density with χ at distance of $3.5Km$ from the centre of the star.

III. GR EFFECTS

As already mentioned above the energy deposition rate due to the process $\nu\bar{\nu} \rightarrow e^+e^-$ in Newtonian gravity has been studied earlier [7, 8]. The energy deposited per unit volume per unit time in Newtonian gravity can be given as [6]

$$\dot{q}(r) = \int \int f_\nu(p_\nu, r) f_{\bar{\nu}}(p_{\bar{\nu}}, r) [\sigma |v_\nu - v_{\bar{\nu}}| \epsilon_\nu \epsilon_{\bar{\nu}}] \frac{\epsilon_\nu + \epsilon_{\bar{\nu}}}{\epsilon_\nu \epsilon_{\bar{\nu}}} d^3 p_\nu d^3 p_{\bar{\nu}}, \quad (2)$$

where f_ν and $f_{\bar{\nu}}$ are the number densities of neutrinos and antineutrinos respectively in the phase space, v_ν is the neutrino velocity, and σ is the rest frame cross section for the process $\nu\bar{\nu} \rightarrow e^+e^-$. In eqn. 2, we have,

$$[\sigma |v_\nu - v_{\bar{\nu}}| \epsilon_\nu \epsilon_{\bar{\nu}}] = \frac{DG_f^2}{3\pi} (\epsilon_\nu \epsilon_{\bar{\nu}} - p_\nu \cdot p_{\bar{\nu}})^2. \quad (3)$$

The above expression is Lorentz invariant. $G_f^2 = 136 \times 10^{-24} MeV^{-4}$, and $D = 1 \pm 4\sin^2\theta_W + 8\sin^4\theta_W$. Here $\sin^2\theta_W = 0.23$. We will consider the plus sign only in the expression of D since this corresponds to the $\nu_e\bar{\nu}_e$ pairs. It has been assumed that the mass of the electron is negligible. Now we replace $p_\nu = \epsilon_\nu \Omega_\nu$ and $d^3 p_\nu = \epsilon_\nu d\epsilon_\nu d\Omega_\nu$, where Ω_ν is the unit direction vector and $d\Omega_\nu$ is the solid angle. So the rate of energy deposition is

$$\dot{q}(r) = \frac{DG_f^2}{3\pi} \Theta(r) \int \int f_\nu f_{\bar{\nu}} (\epsilon_\nu + \epsilon_{\bar{\nu}}) \epsilon_\nu^3 \epsilon_{\bar{\nu}}^3 d\epsilon_\nu d\epsilon_{\bar{\nu}} \quad (4)$$

where the angular integration is represented by

$$\Theta(r) = \int \int (1 - \Omega_\nu \cdot \Omega_{\bar{\nu}})^2 d\Omega_\nu d\Omega_{\bar{\nu}}. \quad (5)$$

So the energy and angular dependences can be decoupled to make the evaluation simpler.

Let us now consider the effects of GR on this process. The effect of GR on static star was studied by Salmonson and Wilson [7]. In the present paper, we consider the static as well as the rotating star. The GR effect will modify both the energy and angular integrals and will provide us with a new lower limit of integration.

Let us first consider the path of a zero mass particle, *i.e.* a null geodesic. For the metric considered here, one gets,

$$\left(\frac{1}{r^2 e^{\gamma-\rho}} \frac{dr}{d\phi}\right)^2 = \frac{1}{b^2} \frac{1}{e^{2\alpha}(e^{\gamma+\rho} - e^{\gamma-\rho} r^2 \omega^2)} + \frac{1}{b} \frac{2\omega}{(e^{\gamma+\rho} - e^{\gamma-\rho} r^2 \omega^2)} - \frac{1}{e^{2\alpha}} \frac{1}{r^2 e^{\alpha-\rho}}, \quad (6)$$

where r is the distance from the origin, ϕ is the latitude and b is the impact parameter. From the above equation, one can immediately see that the geodesic explicitly depends on the gravitational potentials *i.e.* on the EOS and the frequency of rotation. If we now follow the technique used by [7] and express this equation in terms of the angle θ between the particle trajectory and the tangent vector to the circular orbit, we get

$$\left(\frac{dr}{d\phi}\right)^2 = \tan^2\theta \frac{e^{\gamma-\rho} r^2}{e^{2\alpha}}. \quad (7)$$

If the above expression is substituted in eqn. (6), we get a quadratic expression for b .

$$b^2 - \frac{2\omega r^2}{e^{2\rho} - r^2 \omega^2} b - \frac{r^2}{e^{2\rho} - r^2 \omega^2} = 0. \quad (8)$$

This equation can be solved to get

$$b = \frac{\omega r^2 \pm r e^\rho}{e^{2\rho} - r^2 \omega^2}. \quad (9)$$

b will be same for all the points lying on the same orbit. The above equation also implies a minimum photosphere radius, which we would denote by R , below which a massless particle (neutrino) emitted tangentially to the stellar surface ($\theta_R = 0$) would be gravitationally bound.

To carry out the angular integral in eqn. (5), we define $\lambda = \sin\theta$, and express the solid angle Ω as

$$\Omega = [\lambda, (1 - \lambda^2)^{\frac{1}{2}} \cos\phi, (1 - \lambda^2)^{\frac{1}{2}} \sin\phi] \quad (10)$$

$$d\Omega = \cos\theta d\theta d\phi. \quad (11)$$

Using the same notation, we further obtain

where λ_ν and $\lambda_{\bar{\nu}}$ are for neutrinos and antineutrinos respectively, and

$$x(r) = \sqrt{1 - \left(\frac{R}{r}\right)^2 \frac{e^{2\rho} - r^2\omega^2}{e^{2\rho_R} - R^2\omega_R^2}} \quad (13)$$

ρ_R being the potential ρ at the photosphere. Carrying out the integration over λ_ν and $\lambda_{\bar{\nu}}$, we get

$$\Theta(r) = \frac{2\pi^2}{3}(1 - x(r))^4(x(r)^2 + 4x(r) + 5). \quad (14)$$

The gravitational effect modifies the temperature in the energy integral. The temperature $T(r)$ in the energy integral eqn. (4) is the neutrino temperature at radius r . The temperature of the free streaming neutrinos at radius r in terms of their temperature at the minimum photosphere radius R can be deduced if we assume that the temperature varies linearly with redshift. Therefore

$$T(r) = \sqrt{\frac{e^{2\rho_R} - R^2\omega_R^2}{e^{2\rho} - r^2\omega^2}} T(R). \quad (15)$$

In order to quantify the total e^+e^- pair energy deposition, we define Q as the integral of \dot{q} over proper volume. Q is a measure of the total amount of energy converted from the neutrinos to e^+e^- pairs over the whole volume per unit time. So the total amount of local energy deposited via $\nu + \bar{\nu} \rightarrow e^+ + e^-$ reaction is given by

$$Q = 2\pi \int_R^{surface} dr \int \dot{q}(r)r^2 \sin\theta \frac{e^{2\alpha+(\gamma-\rho)/2}}{\sqrt{1-v^2}} d\theta. \quad (16)$$

with $v = (\Omega - \omega)rsin\theta e^{-\rho}$, Ω being the rotational velocity of the star and $\frac{1}{\sqrt{1-v^2}}$ is the lorentz factor.

Integration over the radial and angular variable gives us the total energy deposited per unit time by the $\nu\bar{\nu}$ pairs.

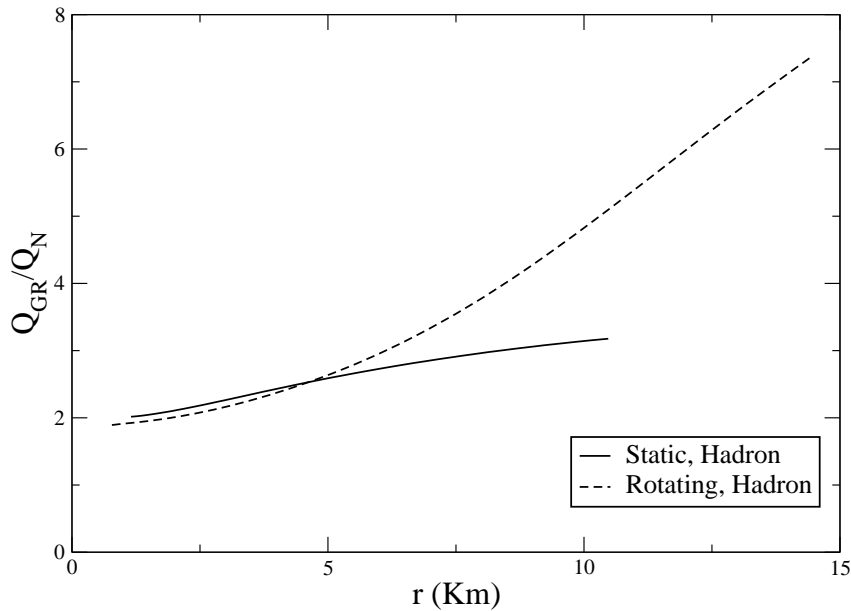


FIG. 4: Variation of the ratio of rate of energy deposition for general relativistic (GR) over Newtonian is plotted along the radial direction, for the hadronic star.

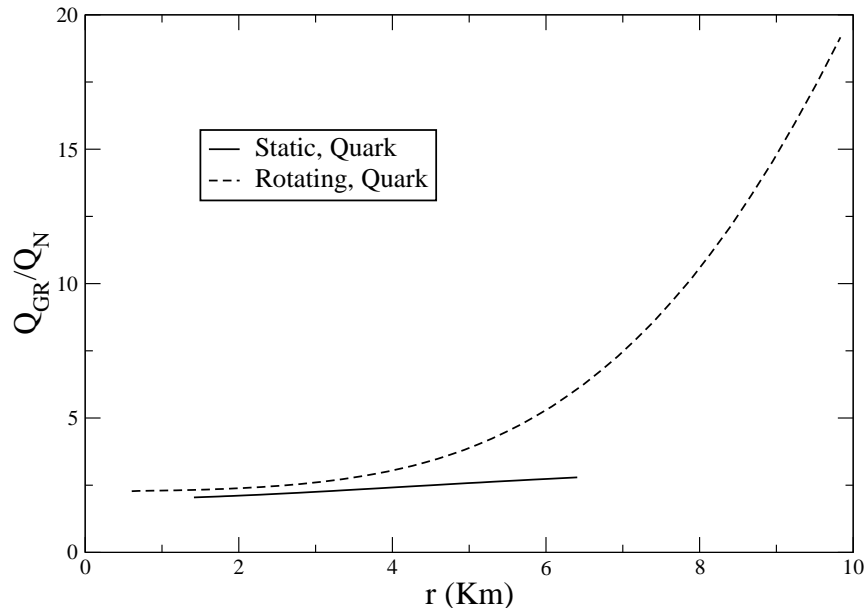


FIG. 5: Variation of the ratio of rate of energy deposition for general relativistic (GR) over Newtonian is plotted along the radial direction, for the quark star.

trapping may increase the temperature considerably inside the star. The eqn. (15) shows that the temperature of the star decreases as we move radially outwards because temperature, like energy, varies linearly with redshift. For the static star, we find that b is minimum for $r = R = 1\text{Km}$ for the hadronic star and $r = R = 1.2\text{Km}$ for quark star. For a rotating star due to high rotational velocity of the star, the shape of the star becomes oblate spheroid. The star is therefore no longer spherically symmetrical and it has an extra deformation parameter to describe its shape. We define this deformation parameter $\chi = \cos\theta$, along the vertical axis of the star. For the EOS, which we have taken the 'rns' code gives the rotational velocity of the star to be $\Omega = 0.62 \times 10^4\text{s}^{-1}$ for the hadronic star and $\Omega = 1.4 \times 10^4\text{s}^{-1}$ for the quark star, the central energy density of both the stars being $1.2 \times 10^{15}\text{gm/cm}^3$. For such a configuration the star deforms to a oblate spheroid but the photosphere is found to be spherical. Photosphere is evaluated by minimising b for different χ . The photosphere radius comes out to be $r = R = 0.78\text{Km}$ for the hadronic star and $r = R = 0.6\text{Km}$ for the quark star.

Figures 4 and 5 depicts the importance of GR on the energy deposition rate both for the static and the rotating compact stars. In both these figures we have divided the radius of the star into small bins of length $100m$ and integrated Q over those bins. The curves in fig. 4 show that for a static star, the energy deposition increases by a factor of 2 at the photosphere. As we go towards the surface the deposition increases and at the surface of the star this ratio becomes little over 3. For the rotating star, at the surface, this ratio is a little less than 8. For the hadronic star the two curves intersect. The ratio for the quark star is about 4 for the static case and reaches a much higher value of 20 at the surface when the star is rotating. From these two figures we conclude that the effect of rotation is to enhance the energy deposition by an order of magnitude both for the quark star and the hadronic star. Moreover, a comparison of the figures 4 and 5 also gives the effect EOS on the energy deposition rate. Since most of the other results are qualitatively similar, in the rest of the paper we will use hadronic star for further discussions.

The figures 6 and 7 show the effect of GR and rotation on the energy deposition rate. In fig. 6 the variation of $\frac{Q_{GR}}{Q_N}$ has been plotted as a function of χ , for different r . Here, one can see that the ratio changes with the polar angle due to rotation. The deposition rate is somewhat pronounced at the pole compared to the equator, mainly near the surface of the star. In fig. 7 we have plotted the total energy deposition rate along the radial direction. The rate of total energy deposition is maximum at the photosphere and it decreases radially outwards, which is implied by the fact that the curves saturate to a maximum limit at higher radius. From this figure one can see that due to rotation the total energy deposition increases by an order of magnitude to 10^{52}ergs/s . It should be mentioned at this stage that the stars (both static and rotating) are constructed with equal central density ($1.2 \times 10^{15}\text{gm/cm}^3$). The rotational velocities for the static and rotating stars are $0.62 \times 10^4\text{s}^{-1}$ and $1.4 \times 10^4\text{s}^{-1}$ respectively.

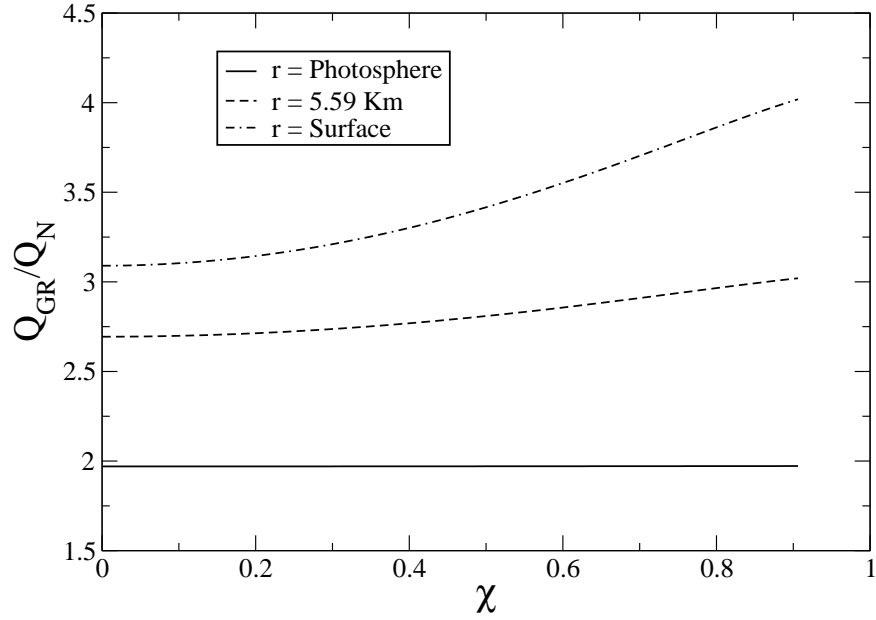


FIG. 6: Variation of the ratio of rate of energy deposition with χ , for three different radial points inside the neutron star.

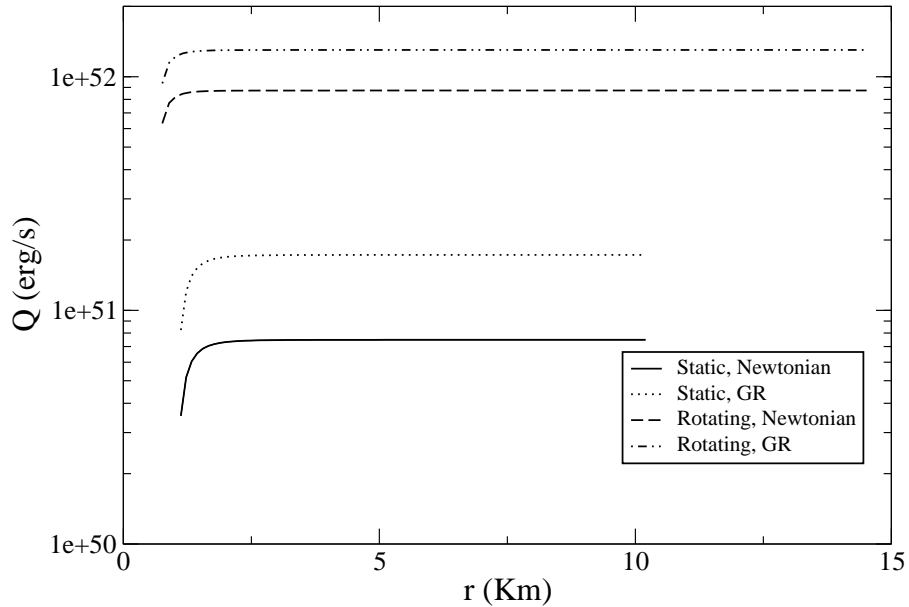


FIG. 7: Variation of rate of energy deposition of general relativistic (GR) and Newtonian along the radius of the static and rotating neutron stars.

mass sequences. The qualitative features remain the same and the quantitative results change only by a few percent. For comparison we should mention that Salmonson and Wilson [7, 8] did the GR calculation for such a reaction on a static star using the Schwarzschild metric. They found that for type II supernova models the enhancement is by a factor of 2 at a rather larger radius $R = 10M$, increasing to a factor of 4 at $R = 5M$, where M being the total mass

argued that 0.5×10^{53} ergs may be liberated from a star in thermal neutrinos within a few seconds [17].

To conclude, we have studied the effect of GR and rotation on the energy deposition rate of the reaction $\nu\bar{\nu} \rightarrow e^+e^-$. The effect of rotation on such a reaction has been considered for the first time. Our findings show that these effects enhance the energy deposition rate by more than an order of magnitude. This finding is very important in the context of describing the GRB associated with a compact, massive, rotating object. In our present calculation we have not considered any neutrino trapping. However the neutrinos may be trapped and raise the temperature of the star [14, 18], thereby further changing the energy deposition rate. Furthermore the consideration of non-equilibrated quark matter rather than equilibrated matter may enhance the energy deposition further. Such studies are in progress.

Acknowledgments

R.M. would like to thank CSIR; New Delhi, for financial support. A.B. would like to thank CSIR; New Delhi, for financial support through the project 03(1074)/06/EMR-II. S.K.G. and S.R thank DST; govt of India, for financial support under the IRHPA scheme.

-
- [1] R. Klebesadel, I. Strong and R. Olsen, *Astrophys. J Lett.* 182 (1973) L85; E. P. Mazets, E. P. Golenetskii and V. M. Ilinskii, *JETP Lett.* 19 (1974) 77
 - [2] C. Kouvelioton *et. al.*, *Astrophys. J Lett.* 413 (1993) L101
 - [3] T. Galama *et. al.*, *Astrophys. J.* 536 (2000) 185
 - [4] J. Hjorth *et. al.*, *Nature* 423 (2003) 847; T. Matheson *et. al.*, *Astrophys. J.* 599 (2003) 394; K. Z. Starck *et. al.*, *Astrophys. J.* 591 (2003) L17
 - [5] J. Goodman, A. Dar and S. Nussinov, *Astrophys. J.* 314 (1987) L7
 - [6] J. Cooperstein, L. J. van der Horn and E. Baron, *Astrophys. J.* 309 (1986) 653
 - [7] J. D. Salmonson and J. R. Wilson, *Astrophys. J.* 517 (1999) 859
 - [8] J. D. Salmonson and J. R. Wilson, *Astrophys. J.* 578 (2002) 310
 - [9] G. B. Cook, S. L. Shapiro and S. A. Teukolsky, *Astrophys. J.* 422 (1994) 227
 - [10] H. Komatsu, Y. Eriguchi and I. Hachisu, *Mon. Not. R. Astron. Soc.* 237 (1989) 355
 - [11] A. Bhattacharyya, S. K. Ghosh, M. Hanauske and S. Raha, *Phys. Rev. C* 71 (2005) 048801
 - [12] N. Stergioulas and J. L. Friedman, *Astrophys. J.* 444 (1994) 306
 - [13] J. Ellis, J. I. Kapusta and K. A. Olive, *Nucl. Phys. B* 348 (1991) 345; Y. Sugahara, H. Toki, *Nucl. Phys. A* 579 (1994) 557
 - [14] S. K. Ghosh, S.C. Phatak and P.K. Sahu, *Nucl. Phys. A* 596 (1996) 670
 - [15] G. J. Mathews and J. R. Wilson, *Astrophys. J.* 482 (1997) 929
 - [16] G. J. Mathews, P. Marronetti and J. R. Wilson, *Phys. Rev. D* 58 (1998) 043003
 - [17] J. R. Wilson, J. D. Salmonson and G. J. Mathews, *AIP Conf. Proc.* 428 (1997) *Gamma-ray Bursts: Fourth Huntsville Symposium*, ed. C. A. Meegan et al. (New York:AIP), 788
 - [18] A. Bhattacharyya, S. K. Ghosh and S. Raha, *Phys. Lett. B* 635 (2006) 195